Computational study of the intramolecular proton transfer reactions of 3-hydroxytropolone (2,7-dihydroxycyclohepta-2,4,6-trien-1-one) and its dimers

Dilara Özbakir Isin · Nihat Karakus

Abstract The proton transfer reaction and dimerization processes of 3-hydroxytropolone (3-OHTRN) have been investigated using density functional theory (DFT) at the B3LYP/6–31+G** level. The influence of the solvent on the proton transfer reaction of 3-OHTRN was examined using the self-consistent isodensity polarized continuum model (SCI-PCM) with different dielectric constants ($\varepsilon =$ 4.9, CHCl$_3$; $\varepsilon =32.63$, CH$_3$OH; $\varepsilon =78.39$, H$_2$O). The intramolecular proton transfer reaction occurs more readily in the gas phase than in solution. Results also show that the stability of 3-OHTRN dimers in the gas phase is directly affected by the hydrogen bond length in the dimer structure.

Keywords Hydrogen bonding · Tropolone derivative · Proton transfer reaction · Dimer

Introduction

Lots of theoretical and experimental studies have been carried out to enhance knowledge of the mechanisms of proton transfer, tautomeric equilibrium and relevant properties, since *intra*- and *inter*molecular proton transfer play key roles in many chemical and biological processes [1–15].

Tropolone and its derivatives have been explored experimentally [16–25] and theoretically [26–32] as model compounds for intramolecular proton transfer. Tropolone (TRN) is a nonbenzoid seven-membered ring

D. Ö. Isin (✉) · N. Karakus
Chemistry Department, Faculty of Science and Literature,
Cumhuriyet University,
58140 Sivas, Turkey
e-mail: dozbakir@cumhuriyet.edu.tr

N. Karakus
e-mail: nkarakus@cumhuriyet.edu.tr

($C_7O_3H_6$). It can act as a hydrogen bond donor or a hydrogen bond acceptor because of its acidic OH proton and its basic C=O groups. Thus, it can form both intramolecular hydrogen bonds and intermolecular hydrogen bonds. The X-ray structure of tropolone shows that the molecules are arranged as centrosymmetric hydrogen-bonded dimers [33, 34]. X-ray diffraction studies show that the hydrogen-bonded dimer is the dominant species in the tropolone crystal, comprising more than 98% of the molecules in the crystal at room temperature (Olender Z, private communication).
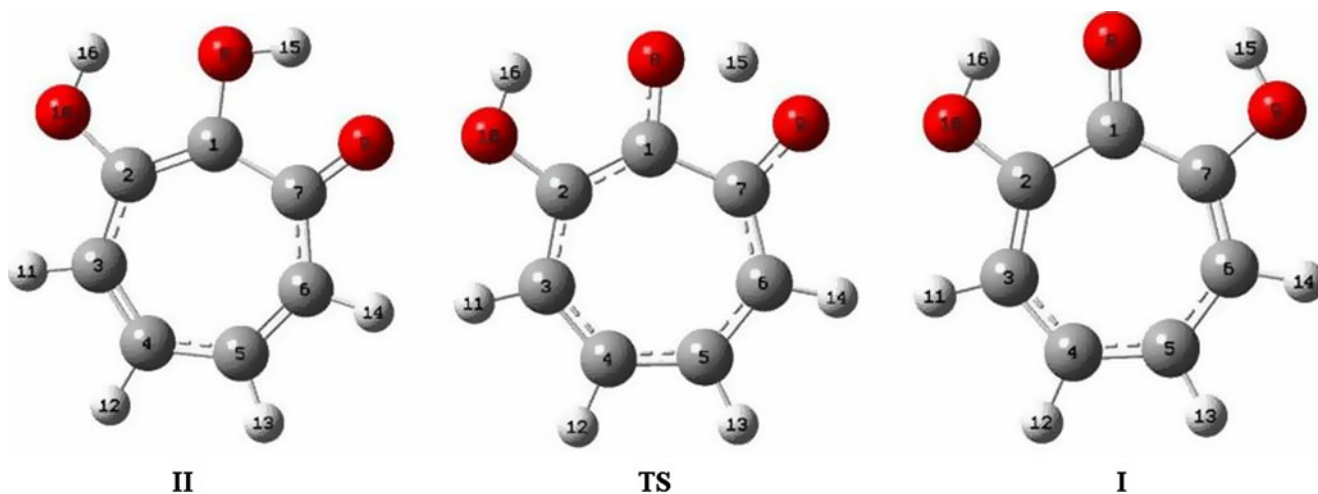
3-OHTRN (3-hydroxytropolone, a derivative of TRN), exhibits two tautomers, 2,7-dihydroxycyclohepta-2,4,6-trien-1-one (I) and 2,3-dihydroxycyclohepta-2,4,6-trien-1-one (II) [35]. In this paper, we report on our investigation of the proton transfer reaction between the I and II tautomers (see Fig. 1) of 3-OHTRN. In this work, we carried out calculations using Becke's three-parameter hybrid functional (B3LYP) methods [36, 37] for 3-OHTRN in chloroform, in methanol and in water in order to evaluate the effect of the solvent on tautomerization. Additionally, computations on 3-OHTRN dimers with two different structures were performed in the gas phase at the same calculation level. Based on a search of the literature, this is the first computational study of the proton transfer reaction between two tautomers of 3-OHTRN and the proton transfer reaction between their dimers. Therefore, we hope that our study provides an enhanced interpretation of tautomers of 3-OHTRN and their dimer structures.

Methods

The stationary structures (I and II) in the proton transfer reaction of 3-OHTRN were optimized using the most

Fig. 1 Optimized molecular structures of I, II and the transition state (*TS*) (obtained using GaussView 3.0 [42])

popular B3LYP [36, 38] method by applying the 6–31+G** basis set with polarization functions on all atoms and diffuse functions on heavy atoms in the gas phase. The vibrational frequencies were obtained at the same level to characterize the local minimum and the transition states (corresponding to a single negative eigenvalue of the Hessian). The basis set superposition error (BSSE) associated with the hydrogen bond energy was computed via the counterpoise method using the individual bases as fragments [39]. In order to take into account the bulk of the solvent, we performed an SCRF calculation using a cavity determined self-consistently from the self-consistent isodensity polarized continuum model (SCI-PCM) [40] with different dielectric constants ($\varepsilon=4.9$, $CHCl_3$; $\varepsilon=32.63$, CH_3OH; $\varepsilon=78.39$, H_2O). All the calculations were performed with the Gaussian 03W computational package [41].

Discussion

The B3LYP/6–31+G** optimized geometries for I, II and TS (the transition state) are shown in Fig. 1, and selected structural parameters are listed in Table 1.

The proton transfer reaction II → TS → I was considered. The transfer of a hydrogen atom from the O_8 to the O_9 atom is accompanied by a rearrangement of the seven-membered ring, and substantial changes are observed in the carbon–oxygen and oxygen–hydrogen bonds. The distance between O_9 and H_{15} decreases upon the proton transfer II → TS → I. The O_8–H_{15} and O_9–H_{15} distances for TS are 1.194 Å and 1.282 Å in the gas phase. It can be concluded that the O_8–H_{15} bond is broken and an O_9–H_{15} bond is formed during the proton transfer process in 3-OHTRN. In the proton transfer II → TS → I, the C_1–C_7 and C_1–C_8 distances decrease, the C_7–C_9 and C_1–C_2

distances increase, while the angle $O_8C_1C_7$ first decreases and then increases in all phases. The $C_1O_8H_{15}$ angle decreases on II → I transfer, while the $C_7O_9H_{15}$ angle increases in all phases.

Let's see how the calculated tautomerization energy for 3-OHTRN changes. The tautomerization energy, as shown in Fig. 2, was calculated as the energy differences between the tautomers and the transition states. The energy differences between the two tautomers (I and II) were calculated to be −5.52, −4.73, −4.42, −4.38 kcal mol⁻¹ in the gas phase, in chloroform, in methanol, and in water, respectively. That is, tautomer I is more stable than tautomer II in the gas phase and in solution.
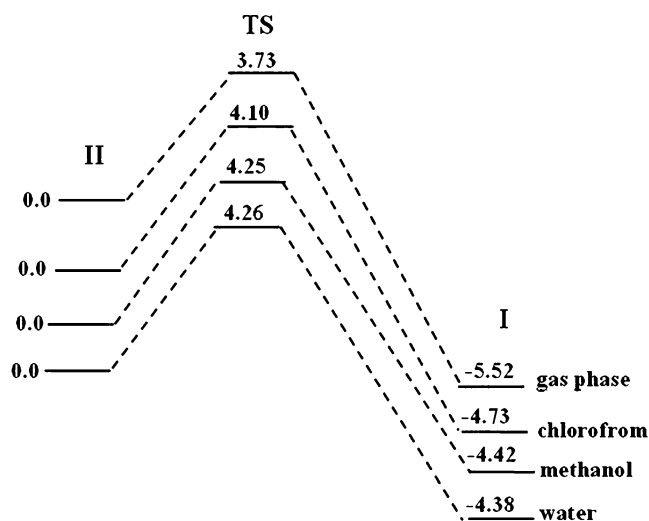
The relative energies of the TS with respect to tautomer II were calculated to be 3.73, 4.10, 4.25 and 4.26 kcal mol⁻¹ in the gas phase, in chloroform, in methanol, and in water, respectively. The barrier height decreases on going from the water phase to the gas phase. As a result, the intramolecular proton transfer reaction between structures I and II occurs more easily in the gas phase than in solution. Similar barrier heights were observed for all of the solutions. However, we can conclude that the stronger the dipole moment of the solvent, the higher the barrier to the proton transfer process.

From the viewpoint of valence theory, the interaction between the lone pair of the acceptor O atom and O–H σ* orbitals is mainly responsible for the proton transfer. Therefore, the O…H–O angle and the O…H distance (in tautomer II) may play important roles in the proton transfer reactions. In most cases, hydrogen bonds with linear O…H–O structures and short hydrogen bond distances are considered to be strong. In tautomer II, the O_8–H_{15}…O_9 angles are 122.80°, 121.98°, 121.69° and 121.61° in the gas phase, in chloroform, in methanol, and in water, respectively. Additionally, the O_8–H_{15}…O_9 hydrogen bond distances of tautomer II are 1.820 Å, 1.842 Å, 1.851 Å and

Table 1 Selected bond lengths, bond angles and dihedrals as derived from B3LYP (6-31+G**) geometric optimization of 3-OHTRN in the gas phase and in solution

Parameters[a]	Gas phase			Chloroform ($\varepsilon=4.9$)			Methanol ($\varepsilon=32.63$)			Water ($\varepsilon=78.39$)		
	I	TS	II	I	TS	II	I	TS	II	I	TS	II
Bond length												
C_1C_7	1.449	1.459	1.462	1.447	1.456	1.459	1.446	1.455	1.457	1.446	1.455	1.457
C_1C_2	1.449	1.400	1.384	1.447	1.400	1.386	1.446	1.401	1.387	1.446	1.401	1.387
C_7O_9	1.347	1.292	1.259	1.350	1.299	1.263	1.351	1.302	1.266	1.351	1.302	1.266
C_1O_8	1.266	1.310	1.350	1.270	1.313	1.352	1.270	1.314	1.352	1.271	1.314	1.352
C_2O_{10}	1.347	1.359	1.363	1.350	1.359	1.362	1.351	1.358	1.362	1.351	1.358	1.362
$O_{10}H_{16}$	0.983	0.974	0.971	0.983	0.973	0.972	0.983	0.973	0.972	0.982	0.973	0.972
O_9H_{15}	0.983	1.282	1.820	0.983	1.273	1.842	0.983	1.269	1.851	0.982	1.269	1.852
$O_8\ldots H_{15}$	1.919	1.194	0.994	1.931	1.198	0.991	1.936	1.200	0.990	1.937	1.200	0.990
$O_8\ldots H_{16}$	1.919	2.126	2.074	1.931	2.151	2.086	1.936	2.162	2.090	1.937	2.162	2.093
Bond angle												
$O_8C_1C_7$	117.63	109.35	112.37	117.72	109.44	112.73	117.76	109.47	112.89	117.76	109.47	112.89
$O_8C_1C_2$	117.63	120.65	116.23	117.72	120.84	116.07	117.76	120.92	115.96	117.76	120.90	116.00
$C_1C_2O_{10}$	112.66	116.68	117.91	112.78	116.90	117.99	112.81	117.00	118.01	112.84	117.00	118.05
$C_1C_7O_9$	112.66	108.83	114.66	112.78	108.69	114.77	112.81	108.64	114.85	112.84	108.63	114.82
$C_7O_9H_{15}$	105.14	—	—	105.45	91.71	87.06	105.64	—	—	105.64	—	—
$C_2O_{10}H_{16}$	105.14	107.76	108.74	105.45	108.57	109.53	105.64	108.92	109.83	105.64	108.95	109.92
$C_1O_8H_{15}$	—	—	102.90	84.45	91.90	103.46	—	—	103.64	—	—	103.72
$O_8H_{15}O_9$	120.05	137.83	122.80	119.60	138.26	121.98	119.34	138.43	121.69	119.33	138.45	121.61
Dihedrals												
$O_8C_1C_2C_3$	179.97	-180.00	180.00	-180.00	-180.00	180.00	180.00	-180.00	-179.97	-180.00	-180.00	-0.003
$O_8C_1C_7O_9$	0.035	-0.005	-0.006	-0.0012	-0.002	0.0160	0.010	-0.003	0.031	-0.026	-0.003	0.027
$C_1C_2O_{10}H_{16}$	-0.006	0.000	0.002	0.0004	0.0004	-0.0020	-0.001	0.00	0.045	0.004	0.000	-0.003
$C_1C_7O_9H_{15}$	0.006	—	—	-0.0004	0.0010	-0.0190	0.001	—	—	0.004	—	—

[a] Distances in Å; angles in degrees. For numbering of atoms, see Fig. 1

Fig. 2 Energy diagram of the proton transfer process in various solvents (via SCI-PCM) and in the gas phase

1.852 Å in the gas phase, in chloroform, in methanol, and in water, respectively. The existence of a strong O_8–H_{15}…O_9 hydrogen bond in tautomer II shows that the barrier to the intramolecular proton transfer may have be low in the gas phase. Another reason for this result is that the distance of O_8 from H_{15} in the TS structure is shortest in the gas phase.

Let's now examine the calculated relative free energies (ΔG) and activation free energy barriers ($\Delta G^{\#}$) for the proton transfer reaction of 3-OHTRN in the gas phase and in solutions. As seen in Table 2, the free energy for the proton transfer reaction of 3-OHTRN is lowest in the gas phase. The activation free energy barrier height decreases on going from the water phase to the gas phase. As a result, according to ΔG and $\Delta G^{\#}$, this reaction is thermodynamically and kinetically easier in the gas phase than it is in solution.

When we look at the calculated ΔE_s and ΔG_s values in Table 3, we see that tautomer II is the more stable of the tautomeric structures, presumably due to solvent effects. In addition, solvents effects mean that the TS structure in solution is more stable than it is in the gas phase. Consequently, the energy barrier to proton transfer reaction increases in solution.

Table 2 Calculated free energies and activation free energy barriers (in kcal mol^{-1}) for the proton transfer reaction of 3-OH-TRN

	ΔG	$\Delta G^{\#}$
Gas phase	−5.15	1.74
Chloroform	−4.42	2.11
Methanol	−4.13	2.25
Water	−4.08	2.28

Dimers

The structural parameters of the dimer structures (I-D and II-D) calculated at the B3LYP/6-31+G** level are shown in Fig. 3.

The optimized geometrical parameters indicate that the two tautomers (I and II) are fully planar, in agreement with experimental values [43]. The planarity of these structures is attributed to the strong intramolecular hydrogen bonding and the structure of the tropolone ring.

A study of the crystal structure of 3-OHTRN has shown that the O_9–H_{15}...O_8 hydrogen bond length is 1.930 Å, the O–H...O angle is 122.4°, and the C_1–O_8 and C_7–O_9 bond lengths are 1.263 Å and 1.346 Å [43]. The calculated O_9–H_{15}...O_8 hydrogen bond length and the O_9–H_{15}...O_8 angle are 1.919 Å and 120.05°, respectively, for tautomer I in the gas phase. The calculated C_1–O_8 and C_7–O_9 bond lengths are 1.263 Å and 1.347 Å, respectively, in the gas phase (see Table 1). These calculated values are in good agreement with the experimental data.

Two tautomer I structures are bonded to each other with two intermolecular hydrogen bonds in the I-D structure [43], while two tautomer II structures are bonded to each other with two intermolecular hydrogen bonds in the II-D structure. These two hydrogen bonds in the dimer structures are equivalent to each other (see Fig. 3).

Comparing the monomer and dimer structures in the gas phase, it has been noted that the intermolecular hydrogen bonds affect the molecular structure of the monomer. As seen in Table 1 and Fig. 3, the bond angles and lengths of the hydrogen donor (O–H) and hydrogen acceptor (C=O) groups of the I-D and II-D structures differ from those of their monomers. For example; the $C_2O_{10}H_{16}$ and $O_8C_1C_2$ angles are increased by 7.38° and 1.90° in I-D, respectively. The $C_1O_8H_{15}$ and $C_1C_7O_9$ angles are increased by 11.67° and 2.87° in II-D, respectively. Another important point is the changes in the C_1O_8 (C_7O_9) and $O_{10}H_{16}$ (O_8H_{15}) bond lengths on going from the monomers to the dimeric structures. The results obtained for the gas phase show that the C_1O_8 and $O_{10}H_{16}$ bond lengths are 0.003 Å longer in I-D. The C_7O_9 and O_8H_{15} bond lengths are 0.001 Å shorter in II-D. Additionally, there are changes in the intramolecular hydrogen bonds on going from the monomers to the dimeric structures. The O_8…H_{16} hydrogen bond lengthens by 0.252 Å, while the O_8…H_{15} hydrogen bond shortens by 0.046 Å in I-D. The O_9…H_{15} hydrogen bond lengthens by 0.393 Å, while the O_8…H_{16} hydrogen bond shortens by 0.113 Å in II-D.

The values of the calculated uncorrected interaction energies, ΔE, and the corrected interaction energies, ΔE_c, are given in Table 4. The interaction energies are corrected for basis set superposition error (BSSE) at the B3LYP level

Table 3 Dipole moments (μ, in debyes), solvation energies $\Delta E_s = E_{gas} - E_{solv}$, and solvation Gibbs free energies $\Delta G_s = G_{gas} - G_{solv}$ (kcal mol^{-1}) of the tautomeric forms in the gas phase and in solution

	Gas phase	Chloroform			Methanol			Water		
	μ	ΔE_s	ΔG_s	μ	ΔE_s	ΔG_s	μ	ΔE_s	ΔG_s	μ
I	3.12	−3.34	−3.62	3.94	−4.56	−4.97	4.23	−4.71	−5.13	4.26
II	3.14	−4.13	−4.36	3.96	−5.67	−6.00	4.27	−5.84	−6.20	4.30
TS	3.54	−3.76	−3.99	4.51	−5.15	−5.67	4.88	−5.32	−5.67	4.92

using an approximation to the Boys–Bernardi counterpoise method [39], as described below.

The hydrogen-bonding interaction energy, ΔE, of the dimer (for example I-D) is defined as

$$\Delta E = E_{I \cdots I} - E_I - E_I, \qquad (1)$$

where $E_{I \cdots I}$ refers to the energy of the I-D, and E_I is the energy of tautomer I. When the BSSE is taken into account, the BSSE-corrected interaction energy, ΔE_c, is then calculated as

$$\Delta E_c = E_{I \cdots I} - E_{I(I \cdots I)} - E_{I(I \cdots I)} \qquad (2)$$

where $E_{I(I \cdots I)}$ is the energy of monomer I obtained with the extra ghost Gaussian functions placed at the positions of monomer I in the dimer.

As seen from these calculated interaction energies, II-D is more stable than I-D. When we look at the calculated ΔG values in Table 4, II-D is more stable than I-D by 1.57 kcal mol^{-1}. It is interesting that the intermolecular hydrogen bond lengths in II−D are shorter than those in the
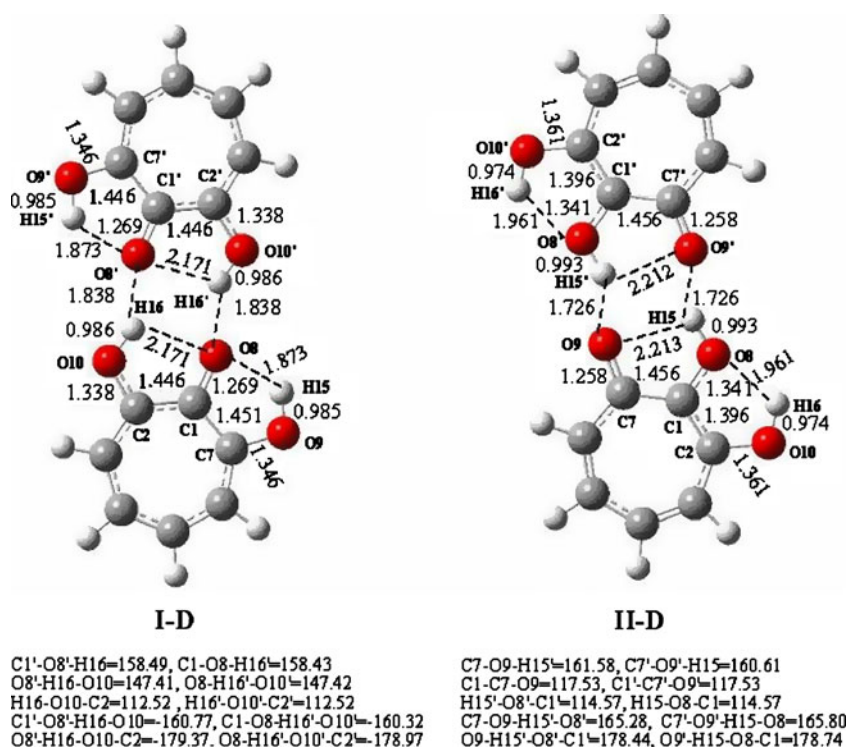
I-D structure. Thus, the stabilities of the dimer structures under investigation can explain the intermolecular hydrogen bonds formed in the dimers.

Conclusions

The major conclusions to be gleaned from this work are as follows:

1. Tautomer I is more stable than tautomer II in the gas phase and in solution.
2. The barrier height for the proton transfer reaction of 3-OHTRN decreases upon shifting from the water phase to the gas phase. As a result, the intramolecular proton transfer reaction between structures I and II is thermodynamically and kinetically easier in the gas phase than in solution.
3. The geometrical parameters of the two monomer molecules in the I-D and II-D structures are nearly the same.

Fig. 3 Optimized structures of the I-D and II-D structures. Bond lengths are shown in Å and angles in degrees (obtained using GaussView 3.0 [42])

I-D

C1'-O8'-H16=158.49, C1-O8-H16'=158.43
O8'-H16-O10=147.41, O8-H16'-O10'=147.42
H16-O10-C2=112.52 , H16'-O10'-C2'=112.52
C1'-O8'-H16-O10=−160.77, C1-O8-H16'-O10'=−160.32
O8'-H16-O10-C2=−179.37. O8-H16'-O10'-C2'=−178.97

II-D

C7'-O9-H15'=161.58, C7'-O9'-H15=160.61
C1-C7-O9=117.53, C1'-C7'-O9'=117.53
H15'-O8'-C1'=114.57, H15-O8-C1=114.57
C7-O9-H15'-O8'=165.28, C7'-O9'-H15-O8=165.80
O9-H15'-O8'-C1'=178.44, O9'-H15-O8-C1=178.74

Table 4 Calculated free energies ΔG, interaction energies ΔE, BSSEs, and corrected interaction energies ΔE_C for the dimerization of tautomers of 3-OHTRN in the gas phase

Structures	ΔE	BSSE	ΔE_c	ΔG
I-D	−6.84	0.91	−5.93	5.28
II-D	−8.45	0.95	−7.50	3.71

4. II-D is more favorable than I-D. That is, the intermolecular hydrogen bonds in the II-D structure are stronger than those in the I-D structure.

5. The results show that the stabilities of the dimer structures are directly affected by the hydrogen bond lengths in the dimer structures.

6. At this time, there are no published data from computational investigations of the intramolecular proton transfer reactions of 3-hydroxytropolone and its dimers, so our calculations provide a useful interpretation of literature data.

References

1. Alves ACP, Hollas JM, Musa H, Ridley T (1985) J Mol Spectrosc 109:99–122
2. Sekiya H, Nagashima Y, Nishimura Y (1989) Bull Chem Soc Jpn 62:3229–3231
3. Yi PG, Liang YH, Tang ZQ (2006) Chem Phys 322:387–391
4. Casadesu's R, Moreno M (2003) Chem Phys 290:319–336
5. Hunter KC, Rutledge LR, Wetmore SD (2005) J Phys Chem A109:9554–9562
6. Yi PG, Liang YH (2006) Chem Phys 322:382–386
7. Nsangou A, Jaidane N, Ben Lakhdar Z (2006) J Mol Struct 758:87–95
8. Ahn DS, Lee S, Kim B (2004) Chem Phys Lett 390:384–388
9. Enchev V, Markova N, Angelova S (2005) J Phys Chem A 09:8904–8913
10. Wang YQ, Wang HG, Zhang SQ, Pei KM, Zheng XM (2006) J Chem Phys 125:214506–214512
11. Sakota K, Okabe C, Nishi N, Sekiya H (2005) J Phys Chem A 109:5245–5247
12. Folmer DE, Poth L, Wisniewski ES, Castleman AW (1998) Chem Phys Lett 287:1–7
13. Folmer DE, Wisniewski ES, Hurley SM, Castleman AW (1999) Proc Natl Acad Sci USA 96:12980–12986
14. Guallar V, Batista VS, Miller WH (1999) J Chem Phys 110:9922–9936
15. Gorb L, Leszczynski J (1998) J Am Chem Soc 120:5024–5032
16. Ikegami Y (1963) Bull Chem Soc Jpn 36:1118–1125
17. Alves ACP, Hollas JM (1973) Mol Phys 25:1305–1314
18. Redington RL, Redington TE (1979) J Mol Spectrosc 78:229–247
19. Tomioka Y, Ito M, Mikami N (1983) J Phys Chem 87:4401–4405
20. Redington RL, Chen Y, Scherer GJ, Field RW (1988) J Chem Phys 88:627–633
21. Sekiya H, Nagashima Y, Nishimura Y (1990) J Chem Phys 92:5761–5769
22. Sekiya H, Nagashima Y, Tsuji T, Nishimura Y, Mori A, Takeshita H (1991) J Phys Chem 95:10311–10317
23. Nishi K, Sekiya H, Kawakami H, Mori A, Nishimura Y (1998) J Chem Phys 109:1589–1592
24. Frost K, Hagemeister FC, Arrington CA, Zwier TS, Jordan KD (1996) J Chem Phys 105:2595–2604
25. Mó M, Yáñez M, Esseffar M, Herreros M, Notario R, Abboud JLM (1997) J Org Chem 62:3200–3207
26. Redington RL, Bock CW (1991) J Phys Chem 95:10284–10294
27. Sanna N, Ramondo F, Bencivenni L (1994) J Mol Struct 318:217–235
28. Nash JJ, Zwier TS, Jordan KD (1995) J Chem Phys 102:5260–5270
29. Vener MV, Scheiner S, Sokolov ND (1994) J Chem Phys 101:9755–9765
30. Smerdachina Z, Siebrand W, Zgierski MZ (1996) J Chem Phys 104:1203–1212
31. Takada S, Nakamura H (1995) J Chem Phys 102:3977–3992
32. Wójcik MJ, Boczar M, Stoma M (1999) Int J Quantum Chem 73:275–282
33. Shimanouchi H, Sasada Y (1970) Tetrahedron Lett 28:2421–2424
34. Shimanouchi H, Sasada Y (1973) Acta Crystallogr B 29:81–90
35. Tsuji T, Hamabe H, Hayashi Y, Sekiya H, Mori A, Nishimura Y (1999) J Chem Phys 110:966–971
36. Lee C, Yang W, Parr PG (1988) Phys Rev B 37:785–789
37. Becke AD (1993) J Chem Phys 98:5648–5652
38. Becke AD (1988) Phys Rev A 38:3098–3100
39. Boys SF, Bernardi F (1970) Mol Phys 19:553–566
40. Foresman JB, Keith TA, Wiberg KB, Snoonian J, Frich MJ (1996) J Phys Chem 100:16098–16104
41. Frisch MJ et al (2003) Gaussian 03W. Gaussian Inc., Pittsburgh
42. Frisch A, Dennington R II, Keith T, Nielsen AB, Holder AJ (2003) GaussView Reference, v.3.0. Gaussian Inc., Pittsburgh
43. Kubo K, Matsumoto T, Mori A (2007) Acta Cryst E63:o941–o943